Heavy fermion metal–Kondo insulator transition in $FeSi_{1-x}Al_x$

J. F. DiTusa
Department of Physics and Astronomy, Louisiana State University, Baton Rouge, Louisiana 70803

K. Friemelt and E. Bucher
Fakultat fur Physik, University of Konstanz, Postfach 5560, D-78434 Konstanz, Germany

G. Aeppli
NEC, 4 Independence Way, Princeton, New Jersey 08540

A. P. Ramirez
Bell Laboratories, Lucent Technologies, Murray Hill, New Jersey 07974

(Received 22 January 1998)

Doping the Kondo insulator FeSi with Al at the Si site introduces carriers and eventually yields metallic conduction. The lattice constant, thermoelectric effect, Hall effect, electrical conductivity, magnetic susceptibility, specific heat, and magnetoresistance have been measured over the $0<x<0.08$ range of Al concentration. All of these quantities show a systematic variation with x including a metal-insulator transition for carrier densities between 2.2×10^{20} and 4.4×10^{20} cm^{-3}. A detailed analysis of the transport and thermodynamic properties reveal a metal-insulator transition closely resembling that of the classic semiconductors (Si:P, Si:B, and Ge:Sb) with one important exception: a substantially enhanced carrier mass. [S0163-1829(98)11439-X]

I. INTRODUCTION AND MOTIVATION

The transition from an insulator to a metal by the variation of the dopant density or the application of hydrostatic pressure to band insulators and amorphous alloys is one of the most important problems in solids.[1] Metal-insulator investigations in classic semiconductors such as Si and Ge have established that the thermodynamic, transport, and magnetic properties near the transition are determined by both the disorder and the electron-electron interactions.[2,3] Despite the attention to this problem, the realization that both interactions and disorder play central roles has made a theoretical description difficult. One strategy of exploration and for highlighting the role of the Coulomb interactions has been to investigate systems where the electron-electron interaction is expected to dominate. These experiments have focused on the Mott-Hubbard insulators, where the Coulomb interactions are responsible for the insulating behavior, and have resulted in discoveries of metals with interesting magnetic or superconducting ground states. These investigations have found for example, that V vacancies in $V_{2-x}O_3$ produce a metal with spiral magnetic order,[4] Sr substitutions in $La_{2-x}Sr_xCuO_4$ produce a high-temperature superconductor,[5] and hydrostatic pressure applied to $Ni(S,Se)_2$ produces a metal-insulator (MI) transition with novel critical exponents.[6] In recent papers we presented an experimental investigation of the metal-insulator transition induced upon carrier doping FeSi, a strongly correlated, or Kondo, insulator.[7,8] The carrier doping is produced by chemical substitution of Al for Si ($FeSi_{1-x}Al_x$). We found that the ground state of this system is neither magnetic nor superconducting for $0\leqslant x\leqslant0.08$. The MI transition, and the metal that results upon doping, closely resemble Si:P,[2] with only one important distinction, namely, an enhanced quasiparticle mass as indicated by the magnetic susceptibility and specific heat. The purpose of this paper is to present a more thorough rendering of our experiments as well as the results of more recent magnetic-susceptibility and magnetization experiments.

The class of insulators known as Kondo or strongly correlated insulators include some rare-earth intermetallics and the transition-metal compound FeSi.[9–11] These compounds are different from Mott-Hubbard insulators, in that they are correctly predicted by band theory to be insulators without a structural transition, or a doubling of the unit cell. However, the extent to which these insulators are fundamentally different from conventional insulators and semiconductors is unclear.[9] The calculations of the band structure of FeSi, incorporating many-body effects on a mean-field level, find a semiconductor with a band gap (Δ) about twice the experimentally determined value (60 meV).[9,12,13] Measurements of the magnetic susceptibility and inelastic magnetic neutron scattering spectrum revealed thermally activated spin fluctuations which have only recently been modeled by adding a local Coulomb repulsion to the band-structure calculation.[13–15] Clear evidence that this insulator is distinct from the classic band insulators come from measurements of the ac conductivity[16] and the photoemission,[17] which find temperature-dependent features in direct conflict with traditional theories of band-gap insulators.[9] Carrier doping FeSi represents an opportunity to explore a MI transition starting from an insulator in which complex many-body phenomena determine the temperature-dependent transport and magnetic properties. The results of our systematic experiments clearly show that doping this strongly correlated insulator through the MI transition results in a disordered Fermi-liquid ground state with a large carrier mass—a heavy fermion metal. Our data represent convincing support for the proposition that

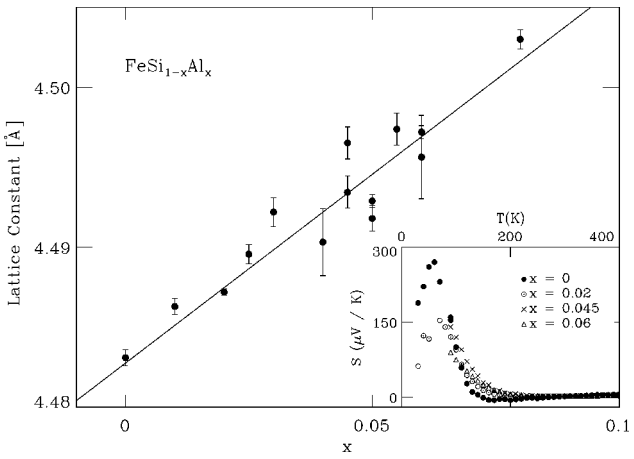

FIG. 1. Lattice constant of $FeSi_{1-x}Al_x$ vs nominal Al concentration (x) determined from powder x-ray-diffraction measurements. Inset: Seebeck coefficient of $Fe_{1-x}Al_x$ for $0 \leqslant x \leqslant 0.06$.

while heavy fermion metals and strongly correlated insulators have peculiar temperature-dependent properties, their ground states remain the well-understood Fermi liquids and band insulators.

We begin our discussion by presenting the details of the experimental techniques that we have used to investigate the MI transition and the extrinsic properties of $FeSi_{1-x}Al_x$. This is followed by a presentation of the experimental results mapping out the broad features of the transition region. The low-temperature transport and thermodynamic quantities are presented and compared to those measured in the classic semiconductors in Secs. IV and V, and we conclude the paper by summarizing our results.

II. EXPERIMENTAL DETAILS

The samples investigated in our experiments were polycrystalline pellets and small bars cut from large single crystals. The polycrystalline samples were produced from high-purity starting materials by arc melting in an argon atmosphere. They were annealed for one week at 1000 °C in evacuated quartz ampoules in order to improve sample homogeneity. Large single crystals were prepared by the Czochralski technique described previously.[18] We employed x-ray spectra of the ground samples obtained with Cu-$K\alpha$ radiation on a SIEMENS D5000 equipped with a position sensitive detector to determine that the samples were single phase. The lattice constant of the doped samples from the x-ray spectra are shown in Fig. 1, where it is apparent that they depend linearly on the Al concentration. This observance of Vegard's law demonstrates that Al successfully replaces Si in the concentration range investigated. We have performed energy-dispersive x-ray microanalysis (EDX) on a JEOL scanning electron microscope equipped with a Kevex Si(Li) detector to check the stoichiometry of our samples. The data show no evidence that the Al, Fe, or Si concentration differs from the nominal values.

The resistance, thermoelectric effect, and Hall-effect measurements were performed on rectangular samples cut by a string saw and polished with emery paper. Thin Pt wires were attached to four contacts made with silver paste which were arranged linearly with an average spacing between voltage probes of 2 mm along an average cross section of 1×0.5 mm^2. The resistivity (ρ) and magnetoresistance (MR) measurements were performed at 19 Hz using standard lock-in techniques in a dilution refrigerator with a 16-T superconducting magnet and a ^{3}He cryostat with a 9-T superconducting magnet. The contacts for the Hall effect were carefully aligned, and measurements were performed at 19 Hz in a gas flow cryostat down to 1.75 K. We performed the Hall measurements with fields between -5 and 5 T taking the Hall voltage (V_H) as $V_H=[V(H)-V(-H)]/2$, thus correcting for any contamination from the field symmetric MR due to misalignment of the contacts.

The magnetic susceptibility (χ) of the same samples was measured in a Quantum Design superconducting quantum interference device magnetometer for fields between 0.1 and 0.5 T and temperatures from 1.75 to 400 K. We collected magnetization measurements at 1.75 K for fields between 0.05 and 5 T. The specific heat was established using a standard semiadiabatic heat pulse technique.

III. EXPERIMENTAL RESULTS

A. Thermoelectric and Hall effect measurements

After establishing that our samples were single phase, and that the Al successfully replaces Si, we determined the concentration and character of the extrinsic carriers by measuring the thermoelectric power and the Hall effect. The Seebeck coefficient (S) shown in the inset to Fig. 1 reproduces the data of Refs. 19 and 20 for the nominally pure sample, changing sign twice between 50 K and room temperature. The peak at ~ 50 K is thought to be due to a phonon-drag mechanism, while the sign changes are due to the competition between the density and mobility of holes and electrons.[19] A thorough description of the Seebeck coefficient for pure and carrier-doped FeSi is given in Ref. 20. The Seebeck coefficient is crucial, as it determines the sign of the carriers for Al-doped samples. Our data show a positive coefficient over the entire temperature range as well as a decreased maximum value, in agreement with the data of Ref. 20. The positive sign of the Seebeck coefficient for the doped samples confirms that the carriers added by Al substitution are predominantly holes as might be expected from the nominal valences of Si and Al.

The Hall resistance (R_H) for a nominally pure single crystal and four Al-doped polycrystalline samples is shown in Fig. 2. R_H was found to be linear in magnetic field for all five samples. The temperature dependence of R_H for the pure sample shows a continuous increase of carrier density with T, consistent with the description of FeSi as a band insulator. It is clear from the figure that at low T the magnitude of R_H is decreased by the chemical substitution. In fact, as the inset to Fig. 2 shows, the apparent carrier concentration ($n = 1/R_H ec$) at 4.2 K is consistent with one hole being donated per added Al atom, thus confirming the carrier doping. In contrast to the low-temperature data, at temperatures above 150 K, R_H of the doped samples is indistinguishable from that of the pure sample. This demonstrates that by 200 K the thermally activated carriers dominate the transport, while at low T the extrinsic carriers added by Al substitution prevail. The T dependence of the doped samples is not

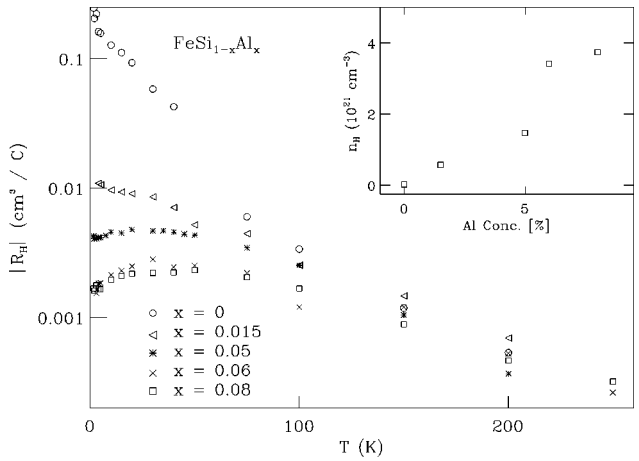

FIG. 2. (a) Hall resistance of $Fe_{1-x}Al_x$ for $0 \leqslant x \leqslant 0.08$. Inset: Nominal carrier concentration calculated from R_H at 4 K for the same samples.

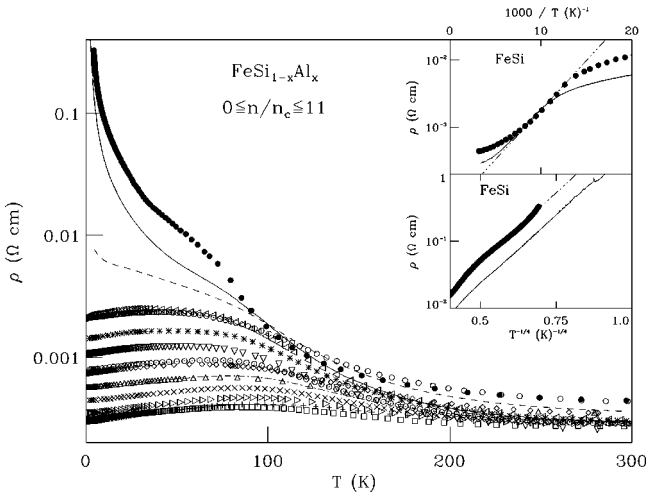

FIG. 3. $\rho(T)$ for $FeSi_{1-x}Al_x$ with x of 0.0 single crystal (●), 0.0 (solid line), 0.005 (dashed line), 0.01 (◁), 0.015 (○), 0.015 (*), 0.025 single crystal (▽), 0.025 (⊙), 0.035 (dashed-dotted line), 0.045 (×), 0.05 (◇), 0.055 (▷), 0.06 (△), 0.07 (+), and 0.08 (□). Top inset: The resistivity of the nominally pure samples plotted as a function of T^{-1} on a log-log scale showing activated behavior (dash-dotted line) over a limited temperature range with $\Delta_\rho = 680$ K. Bottom inset: Resistivity of the nominally pure samples plotted as a function of $T^{-1/4}$ on a log-log scale showing a variable range hopping form ($\rho = \rho_o \exp\{T_o/T\}^{-1/4}$, dash-dotted line) at low temperature.

monotonic, with $x > 0.015$ samples all having a maximum between 20 and 40 K. This maximum in R_H is ubiquitous among doped insulators occurring in Si:P,[21] Ge:Sb,[22] *n*-type GaAs,[23] and $V_{2-x}O_3$,[4] as well as many heavy fermion compounds.[24] In the heavy fermion compounds maxima of the Hall resistance are generally attributed to incoherent magnetic skew scattering, while in the classic semiconductors such maxima have been attributed to either a crossover from conduction to impurity band transport,[25] the presence of discrete localized states degenerate with the conduction band,[23] or an energy-dependent Coulomb scattering.[22]

B. Resistivity measurements

The evolution of resistivity with Al substitution is presented in Fig. 3. For temperatures between 100 and 250 K, a thermally activated form $\rho = \rho_a \exp[\Delta_\rho / 2k_B T]$ describes the pure samples, as can be seen in the top inset to Fig. 3. The dash-dotted line is the best fit to this form resulting in $\Delta_\rho = 680$ K. At temperatures below 50 K the resistivity crosses over to a variable-range-hopping (VRH) form, $\rho = \rho_1 \exp[(T_o/T)^{1/4}]$. Variable-range-hopping transport is due to phonon-assisted hopping, and is prevalent among insulators with a small density of extrinsic carriers. The bottom inset to Fig. 3 presents the conductivity data for the pure samples on a log scale plotted as a function of $T^{1/4}$. Fits of the VRH form to the data yield T_o of 7600 and 8400 K for the two samples, in good agreement with previous measurements of nominally pure samples.[26,27]

The data shown in Fig. 3 for the Al-doped samples reveal that the room temperature ρ is only weakly dependent on x consistent with the thermally activated carriers dominating the transport, as suggested by the Hall data. This observation also demonstrates only minor mobility losses for the carriers due to any disorder induced upon doping. The low temperature ρ, however, shows a much more dramatic and systematic variation with Al substitution. Samples with $x > 0.005$ all have a peak in ρ between 50 and 100 K with metallic behavior, positive $d\rho/dT$, at lower temperatures. The crossover from insulating to metallic low-temperature conductivity occurs at $0.005 < x < 0.01$, indicating a metal-insulator transition at Al concentrations between 2.2 and 4.4×10^{20} cm^{-3}. These metals are very poor conductors with mean free paths (l) estimated from the conductivity and Hall-effect data between 4 and 10 Å at 4 K. This corresponds to an elastic scattering every other unit cell.

The data in Figs. 3, 4, and 5 show just how systematic the changes in ρ with Al concentration are. In Fig. 4(a), we plot the concentration dependence of the temperature at which ρ is a maximum ($T_{\max}$). Here $T_{\max}$ is seen to increase from 30 to 90 K over the range of x studied. The energy gap (Δ_ρ) is measured by fitting an activated form to ρ at temperatures above $T_{\max}$, and presented in Fig. 4(b). In Fig. 5(a), we plot the low-temperature conductivity (σ_{LT}) as a function of doping. All of these quantities show a regular variation with Al substitution consistent with the addition of carriers to a small gap semiconductor.

C. Magnetic susceptibility and magnetization

The magnetic susceptibility (χ) of the nominally pure sample shown in Fig. 6 is compatible with that measured previously.[13,16,27] It is characterized by the appearance of magnetic moments upon warming, and can be described above 70 K by an activated behavior of the form $\chi(T) = (C/T)\exp[-\Delta_\chi / k_B T]$, with $\Delta_\chi = 680$ K and $C = 1.9$ emu K/mol. Thus the energy gap apparent in the susceptibility Δ_χ is the same as that measured from the transport in the same temperature range. The Curie constant C is that associated with $g = 2$ and $s = \frac{3}{2}$. At low temperatures, χ follows a Curie-Weiss-like behavior (inset to Fig. 6) corresponding to 0.6% spin-$\frac{3}{2}$ impurity per formula unit. The variation in χ with Al substitution is also presented in Fig. 6, where $\chi(T)$ is plotted for the 12 Al-doped samples. These plots reveal a susceptibility which is essentially the sum of χ

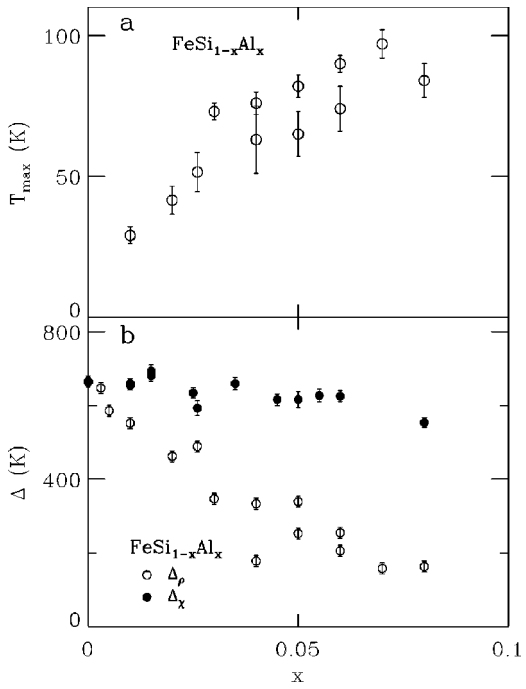

FIG. 4. (a) Temperature dependence of the maximum of the resistivity as a function of Al concentration in $FeSi_{1-x}Al_x$. (b) Energy gap as measured from the resistivity (Δ_ρ) and magnetic susceptibility (Δ_χ) as a function of Al concentration in $FeSi_{1-x}Al_x$.

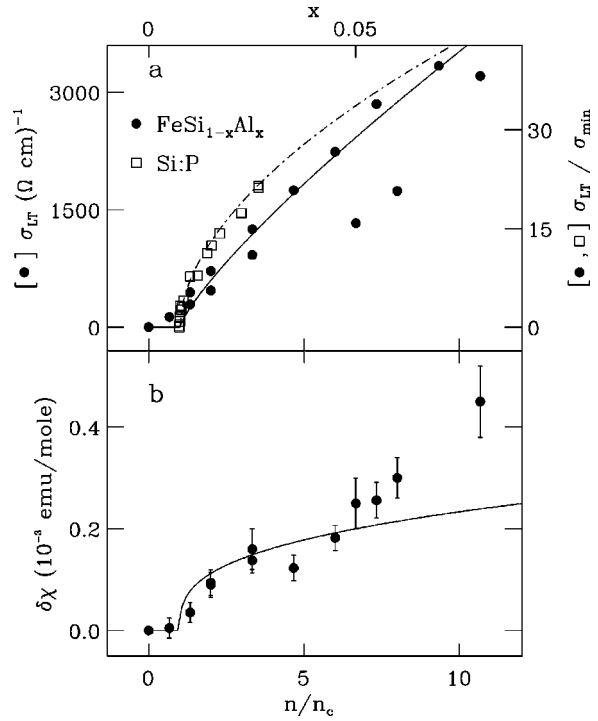

FIG. 5. (a) The low-temperature conductivity of $FeSi_{1-x}Al_x$ vs nominal Al concentration (●). The Si:P data (□, right axis only)(Refs. 31 and 62) are plotted for comparison with $n_c = 3.74 \times 10^{18}$. σ_{min} (right axis) is the Mott minimum conductivity defined as $\sigma_{min} = 0.05 e^2/\hbar d_c$ with $d_c = n_c^{-1/3}$. The solid line represents a fit of $FeSi_{1-x}Al_x$ data up to the concentration where the Ioffe-Regel condition is violated ($k_F l \sim 2$, $x \leq 0.045$) to $\sigma_{LT} = \sigma_o (n/n_c - 1)^\nu$, with a best fit corresponding to $\nu = 0.9 \pm 0.1$ and $\sigma_o = 190 \pm 40\ \Omega^{-1}\,\mathrm{cm}^{-1}$. The dash-dotted line represents the best fit of the Si:P data to the same form ($\nu = 0.55$) (Ref. 2). (b) The change in χ with x, taken as the average χ between 80 and 120 K. The solid line is best fit to the form $\delta\chi = c(n - n_c)^{1/3}$ with $c = 1.44 \mu_B^2 \nu'^{2/3} m^*/\hbar^2 \pi^{4/3}$, where ν' is the valley degeneracy taken as 8 (Ref. 12). The best fit corresponds to a carrier mass of $(14 \pm 1) m_e$.

of the pure sample and a temperature-independent offset ($\delta\chi$). This temperature-independent offset increases with Al concentration, as is evident in Fig. 5(b), where we plot it as a function of x. Since this added susceptibility is both temperature independent and increases with Al concentration, we interpret it as the Pauli susceptibility of the added carriers. That the susceptibility is the sum of a Pauli term and that of the pure sample is further demonstrated in Fig. 4(b), where the x dependence of Δ_χ, found by fitting the activated form added to $\delta\chi$ of the doped samples, is plotted. There is at most a 100-K decrease in $\Delta\chi$ over this range in x. We interpret the small change in Δ_χ as evidence that the addition of itinerant carriers has not significantly altered the gross features of the band structure.

The low temperature χ of all of our doped samples follows a Curie-Weiss form [$\chi = \chi_o/(T - \theta_W)$], as shown for a few samples in the inset to Fig. 6. The Weiss temperature (θ_W) varies from sample to sample from -5 to -50 K, and neither the magnitude of χ_o nor θ_W varies systematically with doping. Furthermore, our data show no signs of a classical magnetic phase transition and in fact follow the Curie-Weiss form to temperatures well below θ_W.

In order to explore the low-temperature magnetic properties of our samples further, the magnetization (M) was measured at 1.75 K for fields up to 5 T. Figure 7 presents $M(H)$ data of seven different Al concentrations. Here again it is apparent that the magnitude of the magnetization does not vary systematically with x. The most naive interpretation of these data would consist of the linear $M(H)$ of the free carriers ($\delta\chi H$) added to the magnetization of noninteracting ions $M_l = n_l g \mu_B J B_J(g\mu_B H/k_B T)$, where n_l is the density of local moments and B_J is the Brillouin function $B_J(x)$

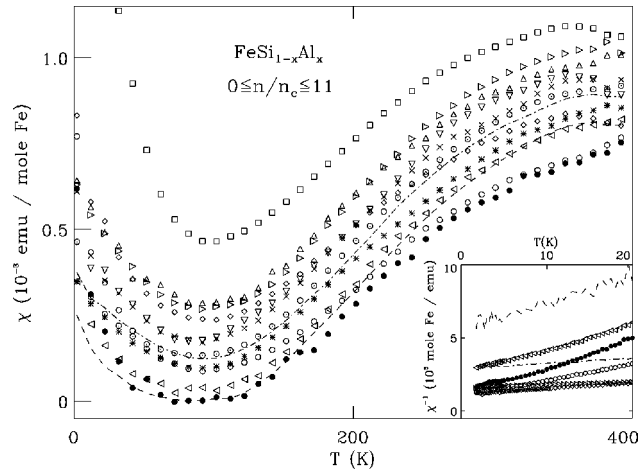

FIG. 6. Magnetic susceptibility [$\chi(T)$] for $FeSi_{1-x}Al_x$ at 0.1 T, with symbols the same as in Fig. 4. Inset: Curie-Weiss plot of the magnetic susceptibility of six $FeSi_{1-x}Al_x$ samples (some samples omitted for clarity).

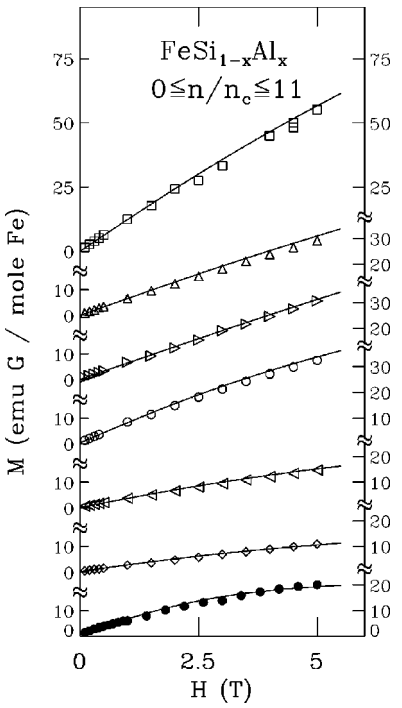

FIG. 7. Magnetization (M) of $FeSi_{1-x}Al_x$ at 1.75 K with x of 0.0 single crystal (●), 0.005 (◇), 0.01 (◁), 0.015 (○), 0.055 (▷), 0.06 (△), and 0.08 (□). Lines represent the Pauli paramagnetic signal determined from the susceptibility as in Fig. 6(b) added to the best fit of the remainder to the model of Bhatt and Lee (Ref. 46).

$=(2J+1/2J)\coth(2J+1/2J)x-(1/2J)\coth(1/2J)x$.[28] Fits of this form to the data using the measured $\delta\chi$ as the Pauli susceptibility require a density of noninteracting ions of $\sim 1\%$ and either a very small gyromagnetic factor ($g<1$) or an angular momentum (J) of the ions of greater than 7. This unsatisfactory outcome of the fits reflects the observation that the $M(H)$ data, even with the linear susceptibility of the free carriers subtracted off, do not saturate in fields of 5 T.

D. Specific heat

Our resistivity data reveal metallic conduction which increases with x in the same samples where χ has an increased doping-induced temperature-independent offset. We have interpreted both these changes as being due to the introduction of free carriers with Al substitution. If this interpretation is correct one would expect a linear-in-T contribution to the specific heat which grows as a function of doping. Figure 8 shows the heat capacity of two Al-doped samples with x's of 0.015 and 0.025. Here the usual method of extracting the linear-in-T contribution (γT) is demonstrated by plotting $C(T)/T$ as a function of T^2. The figure shows that γ of these two samples is much larger than the $\gamma=1.8\times10^{-4}$ J/mol Fe K^2 found in a nominally pure crystal,[27] and that there is also a substantial increase in γ upon going from $x=0.015$ to 0.025 ($\Delta\gamma=2$ mJ/mol Fe K^2). The effective mass of the carriers can be calculated from free electron theory by using $\Delta\gamma$ from the figure and the nominal Al concentration as the carrier concentration. Free-electron theory predicts $\gamma=\pi^2/3\ k_B^2 g(E_F)$ with $g(E_F)=m^*k_F/\hbar^2\pi^2$, and an effective mass of 55 ± 5 times the bare electron mass (m_e). However, band-structure calculations for simple cubic

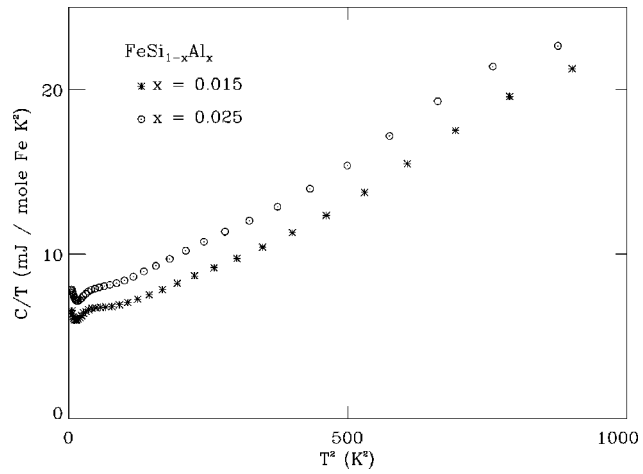

FIG. 8. $C(T)/T$ of $FeSi_{1-x}Al_x$ plotted as a function of T^2 for $x=0.015$ (*) and $x=0.025$ (●).

FeSi, reproduced near the valence-band maximum in Fig. 9, reveal a valence-band maximum along the ΓR line which has a degeneracy (ν') of 8 and a carrier mass of $(1.5\pm0.5)m_e$.[12] The degeneracy reduces our estimate of the effective mass by a factor of $\nu'^{2/3}=4$, resulting in $m^*=(14\pm2)m_e$, still much greater than either the band theory prediction of Fig. 9 or the carrier mass in Si:P or Ge:Sb. A similar analysis for an $x=0.05$ sample prepared at a different time yields $m^*=(17\pm2)m_e$ or $(4.25\pm1)m_e$, with $\nu'=8$. For comparison purposes we have fit the Pauli susceptibility data in Fig. 5(b) to the free-electron theory for a parabolic band which begins to be filled at n_c. We use the form $\delta\chi=(3\pi)^{1/3}\mu_B^2 m^*\nu'^{2/3}[n-n_c]^{1/3}/\hbar\pi^2$, with n_c taken as 0.075. The best fit to our data is shown by the solid line in Fig. 5(b), which represents $m^*=(14\pm2)m_e$, in good agreement with our specific-heat data.

IV. METAL-INSULATOR TRANSITION

From the above discussion it is clear that the lattice constant, thermoelectric effect, Hall effect, resistivity, susceptibility, and specific heat all vary systematically with Al sub-

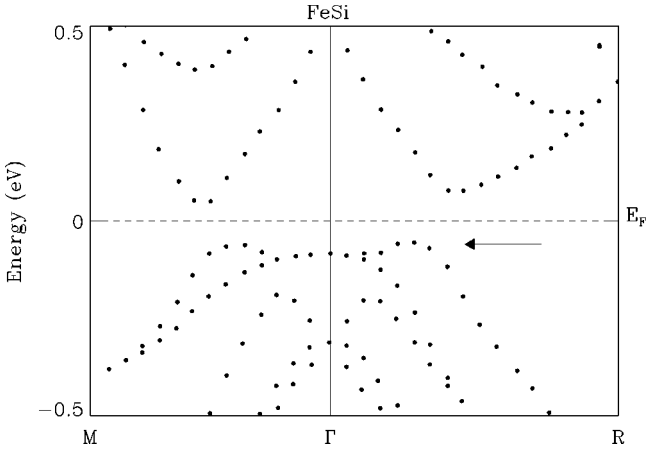

FIG. 9. The band structure of FeSi near the Fermi energy around the valence-band maximum reproduced from the paper by Mattheiss and Hamann (Ref. 12). The valence-band maximum lies between the Γ and R points indicated by the arrow in the figure.

stitution in FeSi. They are all consistent with a transition from an insulating to a metallic state at $x=0.0075\pm0.0025$. Furthermore, we have identified no finite temperature jumps or other singularities in any of these properties, and thus there is no evidence of a structural or magnetic instability in our range of Al substitution. As such we are able to study the details of a continuous metal-insulator transition in this Kondo insulating system, and compare with the extensive literature on the classic semiconductors. This exploration of a quantum phase transition requires careful examination of low-temperature properties close to the MI transition. We present the results of such a systematic investigation in this section.

A. Concentration dependence of the conductivity

The low-T properties of the classic semiconducting systems have been compared in great detail to scaling theories of the transition.[1] In the simplest scaling model the conductivity in proximity to the MI transition has the form

$$\sigma(T,s)=\xi(s)^{-\mu\nu}f[T\tau(s)], \tag{1}$$

where s is a parameter which drives the MI transition.[29] In this case s is the Al concentration. The other parameters in this model are the length scale ξ which diverges as $(s-s_c)^{-\mu}$ and the time scale $\tau(s)$ which diverges as T goes to zero as $(s-s_c)^{-\mu z}$. In these formulas the critical exponent ν is related to the manner in which σ vanishes at $T=0$, $\sigma \propto (s-s_c)^{\nu}$. We begin the comparison of this model with our data by fitting the $\sigma_{LT}(x)$ data in Fig. 5(a) to this standard scaling form [Eq. (1)] with $\sigma_{LT}=\sigma_o[(n/n_c)-1]^{\nu}$. It has been argued that the conductivity follows the form of Eq. (1) in the region where the Ioffe-Regel condition ($k_F l\sim 2$) holds.[2] Therefore, we have restricted the fit to this concentration range, which for our $FeSi_{1-x}Al_x$ samples corresponds to $x\leqslant 0.045$. The best fit for this range in x is shown by the solid line in the figure. The values of ν and σ_o that best represent our data are 0.9 ± 0.1 and $190\pm40\ \Omega^{-1}\,\mathrm{cm}^{-1}$, respectively. In this figure we have also plotted Si:P data from the literature[30] scaled by the Mott minimum conductivity ($\sigma_{\min}=0.05e^2/\hbar d_c$ with $d_c=n_c^{-1/3}$) in order to compare the critical behavior of $FeSi_{1-x}Al_x$ to that of Si:P. The values used to scale the data sets include a critical concentration of $3.87\times10^{18}\ \mathrm{cm}^{-3}$ and a $\sigma_{\min}=20\ \Omega^{-1}\,\mathrm{cm}^{-1}$ for Si:P and $3.3\times10^{20}\ \mathrm{cm}^{-3}$ and $84\ \Omega^{-1}\,\mathrm{cm}^{-1}$ for $FeSi_{1-x}Al_x$. It is clear that the transition region in $FeSi_{1-x}Al_x$ is not as sharp as in Si:P, where it is well documented that $\nu=0.55$.[2] $\nu=0.9\pm0.1$ is closer to the critical behavior in Ge:Sb (Ref. 31) or several other systems [$Ni(S,Se)_2$, GaAs, Si-Au, InO], where $\nu\sim1$.[6,32–34]

B. Temperature and field dependence of the conductivity

In materials on the metallic side of the MI transition the effect of disorder on the temperature and field dependence of the conductivity at low T is significant. This sensitivity results from the diffusive motion of the quasiparticles scattering from the disorder. At low T the vast majority of these scattering events produce little if any change in the phase of the quasiparticle wave function. Thus the phase breaking time (τ_ϕ), the time for the quasiparticle phase to be scattered through 2π with respect to the plane-wave state, is much greater than the elastic scattering time τ. Under these conditions the carriers can retain their phase coherence over many impurity scattering events, resulting in an increased probability of coherent interference of the scattered wave functions. Since these effects arise from the interference of the quasiparticle wave functions, they are known as the quantum contributions to the conductivity.[35–37]

In carrier-doped semiconductors the quantum contributions result in a $\sqrt{T}$ dependence of the conductivity at low temperature.[2,36] This singular behavior has been understood as arising mainly from the electron-electron scattering, and in particular from the diffusion channel of the interaction. The effect stems from the uncertainty principle which requires that two states which differ in energy by ϵ are indistinguishable during a time $\hbar/\epsilon$. Therefore, all scattering within a time $\hbar/\epsilon$ will interfere coherently.[35] Since the motion of the quasiparticles is diffusive, two quasiparticles may encounter each other more than once during this time. The result is an increase in the effective Coulomb coupling constant from λ to $\lambda(1+\alpha_d)$, where α_d is the probability that the two quasiparticles interact more than once in a time $\hbar/\epsilon$.[35] Stated differently, the effective Coulomb interaction is enhanced for diffusive carrier motion since quasiparticles tend to spend more time in a given region of space than the corresponding unscattered plane wave (Bloch) states.[36] This increased coupling constant will enhance both the exchange and direct (Hartree) terms in the self-energy giving rise to a square-root singularity of the density of states at the Fermi level. This singularity is in direct conflict with Landau's idea that in a Fermi liquid the Coulomb interaction renormalizes the density of states, but leaves it a smooth function of energy.[36]

In three dimensions the correction to the conductivity in the diffusion interaction channel is given by

$$\Delta\sigma_I=\frac{e^2}{\hbar}\,\frac{1}{4\pi^2}\,\frac{1.3}{\sqrt{2}}\left(\frac{4}{3}-\frac{3}{2}\tilde{F}_\sigma\right)\sqrt{\frac{k_BT}{\hbar D}}, \tag{2}$$

where $D=v_F l/3$ is the diffusion constant.[36] This equation includes the contributions from the exchange term ($\frac{4}{3}$) and the Hartree term ($3/2\tilde{F}_\sigma$) of the self-energy, where $\tilde{F}_\sigma$ sets the strength of the electron-electron interaction. Figure 10 demonstrates a $\sqrt{T}$ conductivity for four $FeSi_{1-x}Al_x$ samples. The values of m_σ, from fits of our low-T data to the form $\sigma=\sigma_o+m_\sigma T^{1/2}$, are shown in Fig. 11. These m_σ values are similar to those measured in the same range of n/n_c in Si:P ($m_\sigma\sim-3\Omega\ \mathrm{cm\,K}^{1/2}$), Si:B ($m_\sigma\sim-7\ \Omega\,\mathrm{cm\,K}^{1/2}$), Si:As ($m_\sigma\sim-11\ \Omega\,\mathrm{cm\,K}^{1/2}$), and Ge:Sb ($m_\sigma\sim-12\ \Omega\,\mathrm{cm\,K}^{1/2}$).[2,31,38] We also note that in zero field the conductivity of three out of the four samples decreases with increasing temperature (see Fig. 10), requiring $\tilde{F}_\sigma>\frac{8}{9}$.

Moderate magnetic fields have a significant effect on this correction to the conductivity. If we consider the total interference amplitude to be composed of spin singlet and triplet amplitudes, we can understand the effect of the field. In this picture the spin singlet amplitude is not influenced by the field, whereas the states with $j=1$ will be split by $g\mu_B H$. The precession of the spins in the magnetic field causes the interference probability to decrease, effectively cutting off

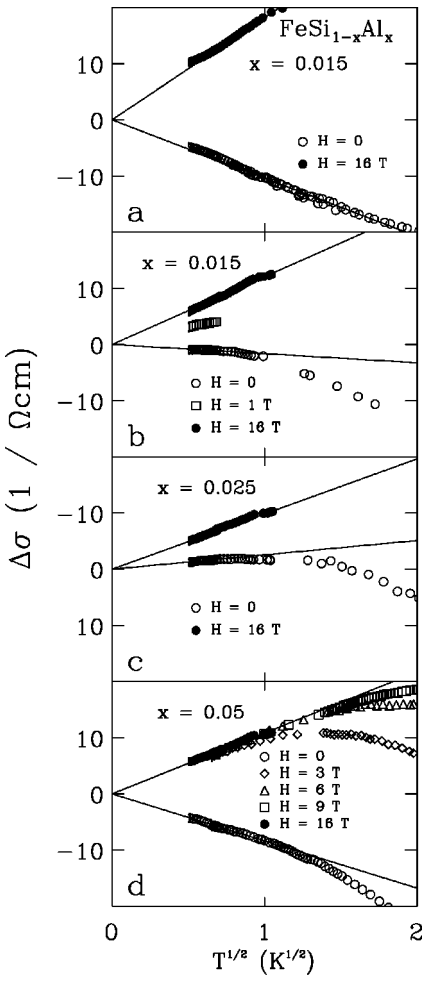

FIG. 10. The change in the conductivity $(\sigma-\sigma_o)$ below 4 K for four Al-doped $FeSi_{1-x}Al_x$ samples plotted as a function of $T^{1/2}$ with $x=0.015$ (a), a second sample with $x=0.015$ (b), $x=0.025$ (c), and $x=0.05$ (d) at zero field (○) and at high field as labeled in the figure. Solid lines represent the best fit of the conductivity to the form $\sigma=\sigma_o+m_\sigma T^{1/2}$ with σ_o and m_σ determined from the fits to the data below 1 K.

the singularity of the triplet terms for $g\mu_B H>k_B T$. Thus there will be field-dependent and -independent contributions to the conductivity resulting in a field and temperature dependence of this contribution of

$$\Delta\sigma_I=\frac{e^2}{\hbar}\frac{1}{4\pi^2}\left[\frac{1.3}{\sqrt{2}}\left(\frac{4}{3}-\frac{1}{2}\tilde{F}_\sigma\right)\sqrt{\frac{k_B T}{\hbar D}}\right.$$

$$\left.-\tilde{F}_\sigma\frac{1}{\sqrt{2}}[1.3+g_3(h)]\sqrt{\frac{k_B T}{\hbar D}}\right], \qquad (3)$$

where

$$g_3(h)=\int_0^\infty d\Omega\,\frac{d^2}{d\Omega^2}[\Omega\,N(\Omega)](\sqrt{\Omega+h}+\sqrt{|\Omega-h|}-2\sqrt{\Omega}),$$

$N(\Omega)=1/(e^\Omega-1)$, and $h=g\mu_B H/k_B T$.[36] g_3 has the limiting behavior

$$g_3(h)=\begin{cases}\sqrt{h}-1.3, & h\gg 1\\ 0.053h^2, & h\ll 1.\end{cases}$$

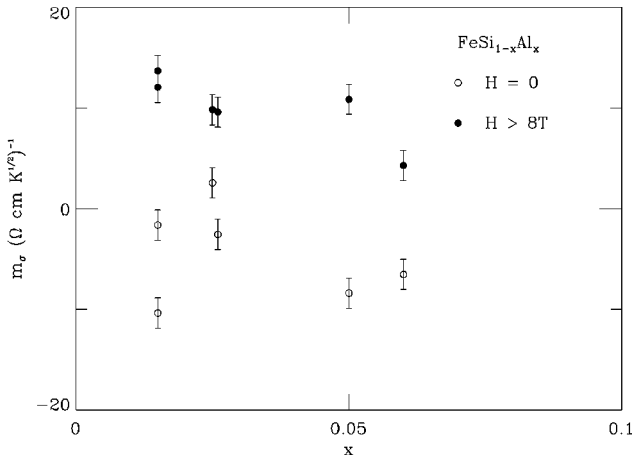

FIG. 11. Plot of m_σ from fits of the low-temperature conductivity to the form $\sigma=\sigma_o+m_\sigma T^{1/2}$ vs the Al concentration of $FeSi_{1-x}Al_x$ in zero field (○), and in high field ($>8T$) (●).

These equations demonstrate that in the theory of electron-electron interactions the exchange term and $\frac{1}{3}$ of the Hartree term are not changed by the magnetic field. Large magnetic fields cut off only the part of the singularity associated with the Hartree term, those in Eq. (2) which include $\tilde{F}_\sigma$, and the relevant field scale is $g\mu_B H\sim\hbar D$.[36]

When examining the magnetoconductance (MC) it is important to recognize two other contributions to the conductivity. The first arises from the Cooper channel interaction, a similar contribution to the diffusion channel interaction described above. In this interaction channel the divergence of the conductivity at low T arises from the Coulomb interaction in much the same way. When discussing the diffusion channel interaction we considered the increase in the Coulomb interaction due to the finite probability that two quasiparticles interact twice during the time $\hbar/\epsilon$ at points A and B. The Cooper interaction channel is similar, except that we consider the case when the path of one of the quasiparticles is time reversed.[35] That is, one quasiparticle diffuses from B to A (time reversed from the A to B path). In this scenario, the two quasiparticles never cross the same region at the same time since one quasiparticle is diffusing in the reverse sense. However, if the time between path intersections is small compared to $\hbar/\epsilon$, then the quantum-mechanical indeterminacy of time allows the wave functions to interfere coherently.[35] This replaces the coupling λ by the effective coupling $\tilde{\lambda}=\lambda/[1+\lambda\ln(E_F/k_B T)]$, a typically a small change since $\lambda\ll 1$. However for superconducting materials $\tilde{\lambda}$ is replaced by $1/\ln(T_C/T)$, where T_C is the superconducting critical temperature, and the interaction is the attractive one which leads to the superconductivity.[35] A magnetic field destroys the time-reversal symmetry, and thus the phase coherence necessary for the effect. A negative MC is predicted when the Landau orbit size becomes comparable to the thermal length, $2eH/\hbar c>k_B T/D$. For all nonsuperconducting materials this term is found be negligible when compared to the diffusion interaction channel.[2,36] Since $FeSi_{1-x}Al_x$ does not show any signs of superconductivity across a wide range of chemical substitution, we have ignored this contribution when analyzing the MC.

At low temperatures the conductivity of disordered mate-

rials can also have contributions from the weak localization of quasiparticles due to coherent backscattering. The origin of this term in the conductivity can be understood by considering two series of scattering events during which the phase of the quasiparticles is not affected by the scattering.[37] In particular we consider two scattering series which have the same changes in momentum but in opposite sequence, $\vec{k} \rightarrow \vec{k}_1' \rightarrow \vec{k}_2' \rightarrow \cdots \rightarrow \vec{k}_{n-1}' \rightarrow \vec{k}_n' \rightarrow -\vec{k}$ and $\vec{k} \rightarrow \vec{k}_1'' \rightarrow \vec{k}_2'' \rightarrow \cdots \rightarrow \vec{k}_{n-1}'' \rightarrow \vec{k}_n'' \rightarrow -\vec{k}$. The first series has momentum changes of $\vec{p}_1, \vec{p}_2, \vec{p}_3, \ldots, \vec{p}_n$ and the second has $\vec{p}_n, \vec{p}_{n-1}, \ldots, \vec{p}_2, \vec{p}_1$. The amplitude for the final state $-\vec{k}$ will be the same since the series undergo the same scattering processes in opposite sequence.[37] The key point is that these two partial waves will interfere constructively, resulting in an increased probability for backscattering. The $-\vec{k}$ direction is the only direction in which the coherent interference results in an increased probability, and this will act to decrease the conductivity at low temperature. In three dimensions the conductivity increases with temperature as $\Delta\sigma_{wl} \propto e^2\ T^{q/2}/\hbar\ \pi^3$, where q is determined by the temperature dependence of the relevant inelastic scattering process.[35]

The effect of a magnetic field on the weak localization term is to induce a phase difference in the two scattering series. In this way a magnetic field will destroy the coherent backscattering if the difference in phase between the two paths is of order π. The magnitude of the phase difference depends on the length and direction of the scattering trajectories. All trajectories with an area projected onto a plane perpendicular to the magnetic field larger than $L_H^2 = \hbar c/2eH$ will have the coherent scattering suppressed.[35] The characteristic field for the suppression is set by the phase breaking scattering time τ_ϕ as $H_\phi = \hbar c/4eD\tau_\phi$. Since the field cuts off the backscattering probability, the MC is positive, and in fields $H \gg H_\phi$ the conductivity has the form[35]

$$\Delta\sigma_{wl} = 0.605 \frac{e^2}{2\pi^2\hbar} \frac{1}{L_H}. \tag{4}$$

In three-dimensional samples of Si:P a small contribution to the MC from the weak localization has been reported. However, this term is dominated by the MC resulting from the diffusion interaction channel, as is typical for three-dimensional samples.[2,39]

The evolution of the conductivity of $FeSi_{1-x}Al_x$ with magnetic field can be seen in Figs. 10 through 13. In large magnetic fields ($h > 1$) our $FeSi_{1-x}Al_x$ samples continue to show a $\sqrt{T}$ divergence. However, as can be seen in Fig. 10, most samples have a sign change in their temperature dependence. This change from metallicliike conductivity (negative $d\sigma/dT$) to insulatinglike (positive $d\sigma/dT$) with the application of magnetic field has been observed in Si:B, Si:P, and Si:As, and results from a large electron-electron interaction constant, $8/9 < \tilde{F}_\sigma < 8/3$.[2] Since there are only two material parameters which determine $\Delta\sigma(T)$ in a constant field [see Eqs. (2) and (3)], $\tilde{F}_\sigma$ and D are fixed by the zero- and high-field temperature dependence. $\tilde{F}_\sigma$ and D varied with Al concentration between 0.7 and 1.2, and 6.3×10^{-3} and 3.8×10^{-2} cm^2/s, respectively. The appearance of a conductivity which evolves in temperature as $\sqrt{T}$ is consistent with the theory of e-e interaction; however, a much more rigorous test lies in the form of the MC. Therefore we have applied $\tilde{F}_\sigma$ and D in examining the MC of these same samples in order to determine if the extrinsic behavior of this unconventional semiconductor can be understood within the conventional theory of a disordered Fermi liquid.

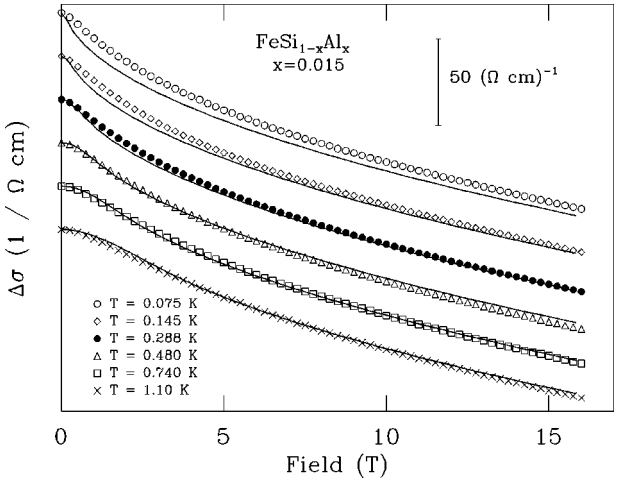

FIG. 12. The magnetoconductance $\sigma(H,T) - \sigma(0,T)$ of $FeSi_{0.985}Al_{0.015}$ as a function of field for various temperatures between 75 mK and 1.1 K. The solid lines represent a fit to all of the temperature- and field-dependent data between 0.75 and 1.1 K for fields up to 16 T to the theory of disordered Fermi liquids (Ref. 36) with three independent parameters: the diffusion constant ($D = 6.3\times10^{-3}$ cm^2/s), the strength of the electron-electron interaction ($\tilde{F}_\sigma = 1.2 \pm 0.1$), and the gyromagnetic ratio ($g = 2.75$).

The MC of two of these four samples can be seen in Figs. 12 and 13 at various temperatures. The MC is negative in all

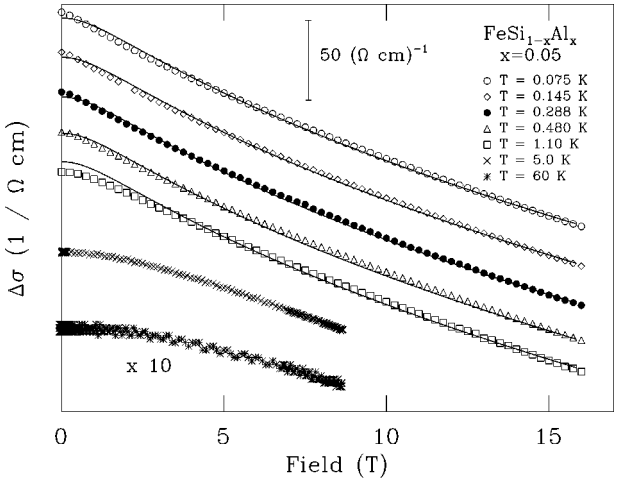

FIG. 13. The magnetoconductance $\sigma(H,T) - \sigma(0,T)$ of $FeSi_{0.95}Al_{0.05}$ as a function of field for various temperatures between 75 mK and 60 K. Solid lines represent a fit to all of the temperature- and field-dependent data between 0.75 and 1.1 K for fields up to 16 T to the theory of disordered Fermi liquids (Ref. 40) with four independent parameters: the diffusion constant ($D = 2.2\times10^{-2}$ cm^2/s), the strength of the electron-electron interaction ($\tilde{F}_\sigma = 1.2 \pm 0.1$), the product of the gyromagnetic ratio and the spin scattering time ($g\tau_s = 7.2\times10^{-12}$ s), and the product of $\sqrt{\tau_s}$ and the density of states [$\sqrt{\tau_s} g(E_F) = 8.8\times10^{16}\sqrt{s}$/eV cm^3].

four samples at all fields at every temperature measured. At low fields the MC varies as H^2, while for fields over 5 T it grows as $\sqrt{H}$. The MC decreases with temperature, although for the sample with $x=0.05$ a negative MC is found for temperatures as large as 60 K. We compare our data with the theory of quantum contributions to the MC which can contain terms from *e-e* interactions in both the diffusion and the Cooper interaction channels, as well as weak-localization effects. In the discussion above we concluded that the contributions from the Cooper interaction channel will be small since there is no indication of superconductivity in this system. The weak-localization terms in the conductivity can also be considered small since the MC measured at high fields is ten times larger and opposite in sign from that predicted in Eq. (4). Therefore, we have ignored these contributions in analyzing the MC data, and instead focused on the diffusive channel of the electron-electron interaction. The contribution to the MC from the diffusion channel interaction can be found from Eq. (3), and has the form

$$\Delta\sigma(H)=-\frac{e^2}{\hbar}\frac{\tilde{F}_\sigma}{4\pi^2}\sqrt{k_BT/2\hbar D}\,g_3(h). \tag{5}$$

For the sample with the smallest conductivity, and thus closest to the MI transition ($x=0.015$), we use $\tilde{F}_\sigma$ and D from the temperature dependence [Eqs. (1) and (2)], and determine g from the high-field MR and Eq. (3) ($g=2.75$). We have plotted the full field dependence of the theoretical prediction of Lee and Ramakrishnan[36] [Eq. (5)] with these three parameters in Fig. 12. We emphasize that this theory, along with the three parameters chosen in the prescribed manner, describes all of our temperature- and field-dependent data below 1.2 K quite well. In this sense the theory of electron-electron interactions does an excellent job of describing the low-temperature transport properties of this sample. However, for the other three samples with larger σ_{LT}, this theory alone cannot reproduce our data. Attempts to follow the same procedure for determining the three parameters (D, $\tilde{F}_\sigma$, and g) produce large values for g, resulting in a grossly overestimated low field MC. We have also varied all the parameters $\tilde{F}_\sigma$, D, and g over a wide range in order to check our procedure and never achieved a satisfactory fit to the data.

Since FeSi is half iron, impurities and defects may act as spin-flip (SF) or spin-orbit (SO) scattering centers. Therefore, we have considered the effect of spin scattering on the predicted MC in order to see if such scattering can explain the apparent discrepancy of electron-electron interaction theory with our data for the samples with larger σ_{LT}. In the theory of the diffusion channel interaction SO and SF scattering mix the spin subbands, effectively cutting off the singularity in the density of states in the same manner as a magnetic field.[36] This effectively reduces the MC especially at low field.[40] In interacting systems a self-consistent field may act to *increase* the MC. This enhanced MC can be seen in our data by comparing the data in Fig. 13 for the sample with $x=0.05$ to the data in Fig. 12 for the sample with $x=0.015$. The comparison shows that the MC of the $x=0.05$ sample becomes larger than that of the $x=0.015$ sample at $H\sim 7$ T. Millis and Lee[40] calculated the MC in the case of strong SO or SF scattering by including both the self consistent field via an effective g factor (g^*), and the reduction of the singularity in the density of states. They wrote the MC as

$$\Delta\sigma=\frac{-2\sigma_o}{3\pi^2}\frac{1}{\sqrt{2\tau_sD}}\frac{1}{g_1(\epsilon_F)\hbar D}[\Psi_3(y)-\Psi_3(0)]. \tag{6}$$

Here,

$$\Psi_3(x)=\frac{3/2(1+\tilde{F}_\sigma/2)}{\tilde{F}_\sigma}\{f((1+\tilde{F}_\sigma/2)x)-f(x)\}$$
$$-\frac{(1+\tilde{F}_\sigma/2)}{\tilde{F}_\sigma}[\{[1+(1+\tilde{F}_\sigma/2)^2x^2]^{1/2}+1\}^{1/2}$$
$$+\{[1+(1+\tilde{F}_\sigma/2)^2x^2]^{1/2}+1\}^{-1/2}]$$
$$+\frac{1}{\tilde{F}_\sigma}[[(1+x^2)^{1/2}+1]^{1/2}+[(1+x^2)^{1/2}+1]^{-1/2}],$$

where $y=g^*\mu_BH\tau_s/\hbar$,

$$f(x)=2[(1+x^2)^{1/2}+1]^{1/2}+\frac{1}{\sqrt{2}}\ln\{[(1+x^2)^{1/2}+1]^{1/2}$$
$$-\sqrt{2}/[(1+x^2)^{1/2}+1]^{1/2}+\sqrt{2}\},$$

$g_1(\epsilon_F)$ is the single spin density of states, σ_o the zero-field conductivity, and τ_s the spin scattering time.[40] We determined $\tilde{F}_\sigma$ and D from the temperature dependence in zero and at 16 T and Eqs. (2) and (3). Equation (6) and a least-squares fitting routine are used to compare this theory to our data. We have performed a three parameter fit to the data at 0.288 K using the products $g^*\tau_s$ and $\sqrt{\tau_s}g_1(\epsilon_F)$ as two of the parameters. Since the theory only holds for $g^*\mu_BH>k_BT$, the low-field data points are ignored in the fit and the zero-field value of the conductivity is taken as the third parameter. At other temperatures (between 0.075 and 1.1 K) $g_1(\epsilon_F)$, τ_s, and g^* are held constant and a one-parameter fit was performed. The best fits found from this procedure are shown by the solid lines in Fig. 13, and the quality of these fits is representative of that for the remaining two samples. The values of the parameters $g^*\tau_s$ and $\sqrt{\tau_s}g_1(\epsilon_F)$ which best reproduce the data are 5.8×10^{-12} s and $5.1\times10^{15}\sqrt{s}/(\mathrm{eV\,cm^3})$ for $x=0.015$, 2.2×10^{-12} s and $1.3\times10^{16}\sqrt{s}/(\mathrm{eV\,cm^3})$ for $x=0.025$, and 7.2×10^{-12} s and $8.8\times10^{16}\sqrt{s}/(\mathrm{eV\,cm^3})$ for $x=0.05$.

The theoretical prediction for a SO relaxation time (τ_{SO}) is proportional to the elastic-scattering time (τ), with $\tau/\tau_{so}=(\alpha Z_i)^4+(\alpha Z)^4$. Here α is the fine-structure constant, Z is the atomic number of the matrix atoms, and Z_i is the atomic number of the impurity species.[41] Since Si, Al, and Fe all have a relatively small Z, τ/τ_{SO} would lie between 2×10^{-4} and 1.3×10^{-3}. The Drude result for the elastic scattering time is ~ 0.1 ps; thus a SO scattering time of ~ 5 ps is a relatively short scattering time. One can also compare these scattering times to the measurements of SO and SF scattering in thin films. In thin-film systems the increased contribution of weak localization to the resistivity has al-

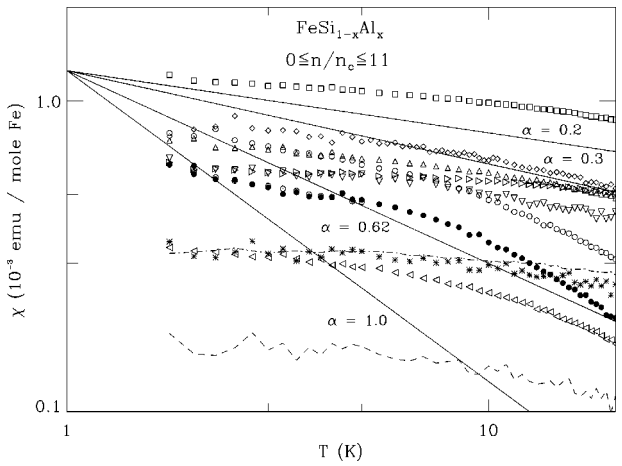

FIG. 14. Magnetic susceptibility $[\chi(T)]$ for $FeSi_{1-x}Al_x$ from 1.75 to 20 K plotted on a log-log scale with the same symbols as in Fig. 4. The solid lines represent various temperature-dependent behaviors with $\chi = T^{-\alpha}$. $\alpha = 1.0$ corresponds to Curie law behavior, and $\alpha = 0.62$ represents the temperature dependence found for Si:P for $n \sim n_c$ (Refs. 45 and 53).

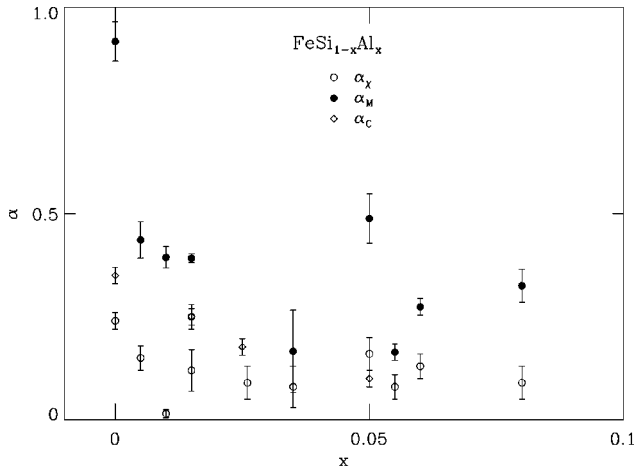

FIG. 15. The parameters α_χ, α_M, and α_C determined from fits to the susceptibility, magnetization, and specific heat of $FeSi_{1-x}Al_x$ at 1.75 K to the theory reference (Ref. 46) .

lowed a systematic measure of these scattering rates as the film surface is varied. For example, Bergmann measured the MC of a 9.2-nm Mg film with $\frac{1}{4}$-ML Au deposited on the top surface and found a SO scattering rate of 5.9×10^{-13} s.[42] Similar Mg films with $\frac{1}{1000}$-ML Fe deposited on the top surface produced a SF scattering rate of 4.7×10^{-12} s.[43] These rates are comparable to the rates we measure in the $FeSi_{1-x}Al_x$ samples. A similar analysis has been carried out for the $Cd_{1-x}Mn_xSe$:In system, where the exchange interaction was found to dominate.[44]

From the quality of the fits describing the low-temperature MC over a wide temperature and field region, we conclude that the temperature and field dependencies of the conductivity are described by the self-consistent electron-electron interaction theory. The only substantial difference that we have found with the behavior of the classic semiconductors is the necessary addition of SF or SO scattering for the majority of our samples.

C. Susceptibility and specific heat

Thus far we have examined the low-temperature behavior of the electrical conductivity of $FeSi_{1-x}Al_x$, and concluded that the description of a disordered Fermi liquid near the MI transition fits our data. Since these aspects of σ are similar to what has been found in common semiconducting systems, we expect that the low-T susceptibility and specific heat of $FeSi_{1-x}Al_x$ and Si:P would also have common temperature and field dependencies. In our discussion of Fig. 6, where we plotted χ of our samples along with a Curie-Weiss-type plot, we remarked that the Curie-Weiss behavior continued down to temperatures below Θ_W. In fact, this is similar to the results of investigations of the classic doped semiconducting system Si:P.[45]

In insulating Si:P the magnetic susceptibility below 1 K diverges much slower than Curie law behavior, and shows no sign of any magnetic phase transitions.[45] This behavior is believed to be due to the broad distribution of exchange interactions between impurity states resulting from the random distribution of dopant atoms. Bhatt and Lee[46] modeled a doped insulator such as Si:P as a random distribution of spin-$\frac{1}{2}$ objects whose magnetic properties are governed by the Heisenberg Hamiltonian

$$H = \tfrac{1}{2}\sum_{i\neq j} J(\vec{r}_i - \vec{r}_j)\hat{S}_i \cdot \hat{S}_j .$$

The exchange is antiferromagnetic, and falls off exponentially with r, $J(r) = J_o \exp -2r/a_B$, where a_B is the Bohr radius of the dopant carrier. Bhatt and Lee investigated this system numerically, simplifying the problem by discarding the high-lying excitation levels of the system which are unimportant at low T. They thus transformed the Hamiltonian to a scaled version which includes only the same low-lying states. The idea is that spins coupled with a $J > T$ will form frozen singlets and drop out of the problem. In this case the susceptibility can be written as $\chi(T) = N_M(T)\chi_c(T)$, where $N_M(T)$ is the effective number of free spins remaining at temperature T, and $\chi_c = \mu_B^2/k_BT$ is the Curie susceptibility of a free spin at temperature T. This model correctly predicted both the slow divergence of χ at low T with $\chi \propto T^{-\alpha}$ and $0 < \alpha < 1$, as well as the lack of a magnetic ordering at low T. Insulating Si:P has thus been described as a random amorphous antiferromagnet where the quantum fluctuations prevent the classically expected spin-glass ordering, giving rise to a random singlet ground state with a divergent susceptibility.

For the Si:P samples doped into the metallic regime, the thermodynamic properties have been interpreted in terms of a two-fluid model, where the localized moments and the itinerant carriers form two independent, weakly interacting systems. The idea is that the local moments are associated with statistically rare regions in the sample which are very weakly coupled to the electron gas. In these regions the coupling to the itinerant electrons is not sufficient to either screen the moments due to the Kondo effect, or to couple moments via Ruderman-Kittel-Kasuya-Yosida interaction.[47–49] The simplest assumption is to take the susceptibility in these rare regions to be of the same form as in the insulating samples. In this case, the susceptibility and specific heat are assumed

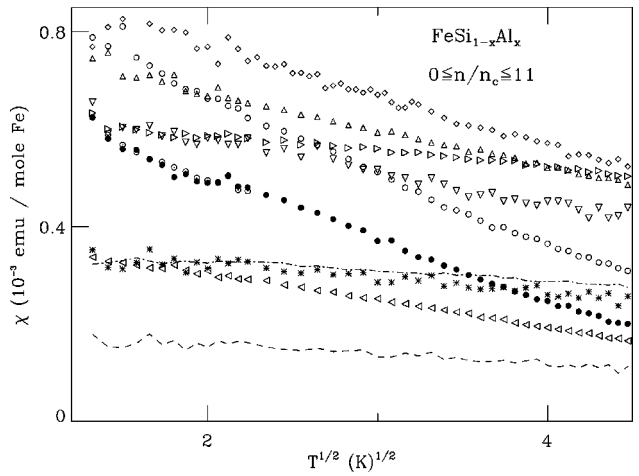

FIG. 16. Magnetic susceptibility $[\chi(T)]$ for $FeSi_{1-x}Al_x$ from 1.75 to 20 K plotted as a function of $T^{1/2}$ on a log-log scale with symbols the same as in Fig. 4.

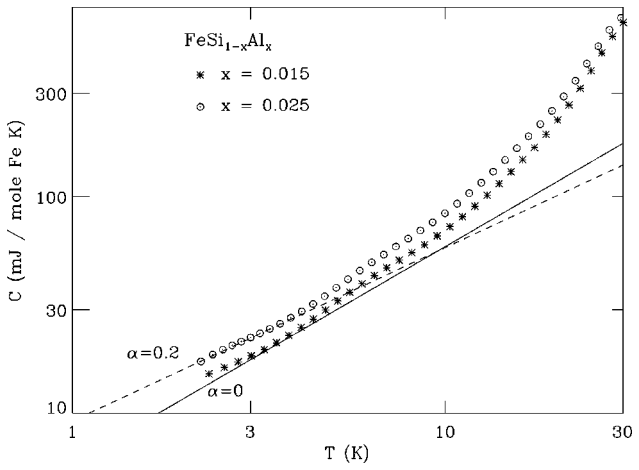

FIG. 17. Specific heat $[C(T)]$ of $FeSi_{1-x}Al_x$ for $x=0.015$ (*) and $x=0.025$ (●). The solid line represents a linear temperature-dependent specific heat expected from a free-electron model $[C(T)=\gamma T]$. The dashed line represents a $T^{1-\alpha}$ dependence with $\alpha=0.2$.

to be the sum of the contribution from the localized spins calculated from the Bhatt-Lee model and the usual Fermi-liquid expressions for the itinerant carriers.[3] Following this procedure and dividing by the Fermi-liquid expressions, the Pauli susceptibility of the itinerant carriers (χ_o) in the case of the susceptibility and the linear specific-heat coefficient of the itinerant carriers (γ_o) for γ, gives susceptibility and linear coefficients of the specific heat[3]:

$$\chi/\chi_o = m^*/m_e + \beta(T/T_o)^{-\alpha},$$

$$\gamma/\gamma_o = m^*/m_e + (T/T_o)^{-\alpha}.$$

Here α is the susceptibility exponent, T_o measures the fraction of impurities which can be described as localized spins, and $\beta = 3.1e^{0.4\alpha}/(1-\alpha)^2$ is the Wilson ratio in the Bhatt and Lee model[46] from fits to the numerical results. This form is not that of a Fermi liquid, since both χ and γ are divergent as $T \to 0$. For Si:P, α was found to be ~ 0.6 for samples very close to the MI transition $(0.78 < n/n_c < 1.25)$.

In order to compare the Si:P results and this theory with our data, we have plotted $\chi(T)$ on a log-log scale in Fig. 14. Here it is clear that $\chi(T)$ diverges much more weakly than either a Curie law ($\alpha=1$) or the data for Si:P ($\alpha \sim 0.6$). The values of α determined from linear fits to the data in the log-log plot (α_χ) are presented in Fig. 15. This figure shows no apparent trend with Al concentration and demonstrates that fits to χ to a power law give α_χ close to 0.2. The data in Fig. 14 diverge very slowly, perhaps slower than the power-law behavior. Such slow divergence has been predicted by models of disordered Kondo systems, which also have the consequence of a non-Fermi-liquid ground state.[47,48] Interestingly, our susceptibility data can be fit equally well by either a Curie-Weiss form or the form $\chi = \chi_a(1-\eta\sqrt{T})$, as can be seen in Fig. 16. A $\sqrt{T}$ dependence of χ is expected from the anomalies in the density of states from electron interactions in a disordered conductor.[50] However, it is not clear from the theory what the magnitude of this contribution to χ should be. This same temperature dependence was reported for Si:P.[51] A $\sqrt{T}$ dependence was also found over a restricted temperature range for the non-Fermi-liquid system $CeCu_{5.9}Au_{0.1}$.[52] The origin of the temperature dependent χ at low T in $FeSi_{1-x}Al_x$ and its relation to $CeCu_{5.9}Au_{0.1}$ is not clear. However, we note that both $CeCu_{5.9}Au_{0.1}$ and $FeSi_{1-x}Al_x$ are close to zero-temperature quantum phase transitions, possibly involving the Kondo screening of local moments.

The temperature and field and dependence of the magnetization of Si:P has been compared in detail to the predictions of the random amorphous antiferromagnet, and found to agree with its predictions.[45] The specific prediction of the Bhatt-Lee model[46] is given by

$$M(H,T) = \frac{k_B T}{g\mu_B}\chi_m(T) f_\alpha(g\mu_B H/k_B T), \tag{7}$$

with $\chi_m(T)$ being the measured low-field susceptibility, and

$$f_\alpha(y) = \left[\int_0^\infty dx \frac{x^{-\alpha_M}\sinh y}{1+e^x+2\cosh y}\right] \Big/ \left[\int_0^\infty \frac{dx\, x^{-\alpha_M}}{3+e^x}\right].$$

We have examined the magnetization of our samples in the spirit of the two fluid model by fitting the sum of Eq. (7) and $\delta\chi H$, the Pauli susceptibility of the metallic samples multiplied by the magnetic field, to our data. The results of this procedure, with a single fitting parameter (α_M), are shown by the solid lines in Fig. 7. In Fig. 15 we plot α_M from the fits that best describe our data. For the Al-doped samples α_M varies from 0.15 to 0.4.

We can also compare this model to the temperature dependence of our specific-heat data. It is clear from the data in Fig. 8 that at low temperatures C/T is not flat, and turns upward below 4 K. In order to characterize C at low temperatures we have plotted it against T on a log-log scale in Fig. 17. The solid line represents the usual linearly dependent specific heat expected for a Fermi liquid. It is clear here again that our data have significant deviations from linear behavior, and are better described by a $T^{1-\alpha_C}$ form with $\alpha_C \sim 0.2$. α_C from linear fits to the low-temperature data on this log-log plot are shown in Fig. 15 along with α_χ and α_M. Although there is significant scatter in the data as well as

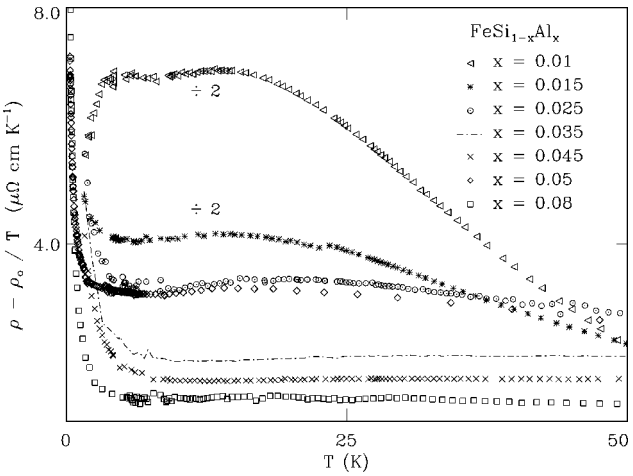

FIG. 18. Change in the resistivity divided by the temperature as a function of the temperature for x between 0.01 and 0.08. ρ_o is determined from a fit of the resistivity to a linear form between 5 and 30 K.

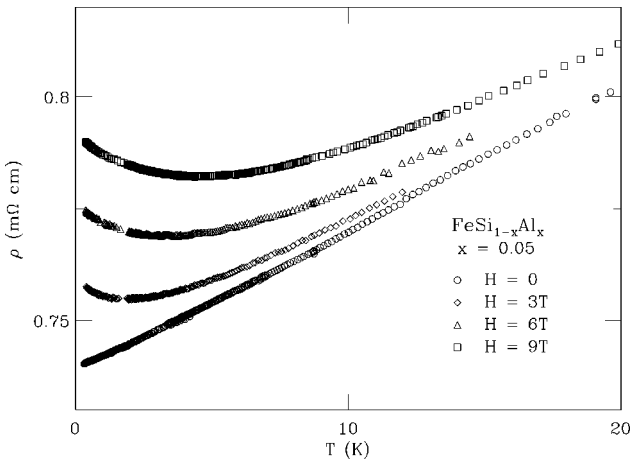

FIG. 19. The resistivity of $FeSi_{0.95}Al_{0.95}$ from 0.3 to 20 K at four magnetic fields (0, 3, 6, and 9 T) exhibiting a linear temperature dependence between 2 and 20 K at $H=0$, and insulating behavior ($d\rho/dT<0$) for high fields at low temperature.

some discrepancy between the values α_χ and α_M, it is clear that the exponent α in $FeSi_{1-x}Al_x$ is much smaller than that found in the Si:P system ($0.5 \leqslant \alpha \leqslant 0.7$).[3,45,51,53] In this sense $FeSi_{1-x}Al_x$ is less magnetic than the classic semiconducting systems, which is surprising in view of the larger dopant density at n_c and the formidable presence of Fe.

V. CROSSOVER FROM LOW- TO HIGH-T BEHAVIOR

In Sec. IV, we showed that the very low-temperature properties of $FeSi_{1-x}Al_x$ are similar to those of the classic semiconducting systems near the MI transition and that the high-temperature properties are dominated by the small gap of the insulating parent compound. We now examine more closely the form of the conductivity in the crossover region between the very low-temperature behavior and that above 100 K. In this crossover region the samples on the metallic side of the MI transition have a linear resistivity over a wide range of temperature and Al concentrations. Figure 18 reveals just how linear the resistivity of our metallic samples is. In this figure we have plotted $(\rho-\rho_o)/T$ against T, with ρ_o chosen from linear fits to the data between 5 and 30 K. A linear ρ would appear as a flat line in this figure, and it is surprising how flat our data are in this temperature range. In Fig. 19 we present ρ for the $x=0.05$ sample which evolves from the low temperature $\sqrt{T}$ behavior to the linear-in-T regime. The field dependence of the resistivity is that due to the electron-electron interactions. The ρ above 1K could be the result of a crossover between the $\sqrt{T}$ behavior and a second contribution; however, the temperature dependence cannot be fit over any significant range by summing a $\sqrt{T}$ form with any power law greater than 1. We have pointed out that these metallic samples have very short mean free paths of order 8 Å. Clearly in such a strong scattering limit Matthesen's rule will be violated, and a more moderate temperature dependence than that found in clean metals would be expected. However, it is not anticipated that a linear-in-T dependence would result from phonon scattering in the limit of strong disorder scattering of the quasiparticles.

A review of the literature on doped Si surprisingly reveals that the linear-in-T behavior is not unique to $FeSi_{1-x}Al_x$. In fact the linearity of the resistivity on the metallic side of the MI transition for a variety of dopants in Si was commented on over 30 years ago by Chapman *et al.*[21] Furthermore, the linearity in the doped Si systems occurs in the same range of n/n_c as $FeSi_{1-x}Al_x$ ($1.25<n/n_c<10$). More recently, linear resistivities have been found in many of the high-T_c superconductors near optimal doping and in rare earth intermetallics such as $U_{0.2}Y_{0.8}Pd_3$,[54] $UCu_{5-x}Pd_x$,[55–57] and $CeCu_{5.9}Au_{0.1}$.[52] For the doped semiconducting systems, the slope $d\sigma/dT$ appears to scale with distance from the MI transition, that is, $\sigma(T,n)=\sigma_1-(n/n_c)\,b\,T$. In Fig. 20 we plot the slope $d\sigma/dT$ vs n/n_c for a number of carrier-doped semiconducting systems, including $FeSi_{1-x}Al_x$, to show the quality of the scaling argument. From the figure it is clear that the coefficient b seems to be a property of the alloy series, ranging from $b=-0.06$ $(\Omega\,\mathrm{cm\,K})^{-1}$ for Si:B, to $b=-8$ $(\Omega\,\mathrm{cm\ K})^{-1}$ for Si:As. What is most striking is that b for $FeSi_{1-x}Al_x$, Si:P, and Si:As is of the same order as b for the Mott-Hubbard insulator and high-T_c superconductor

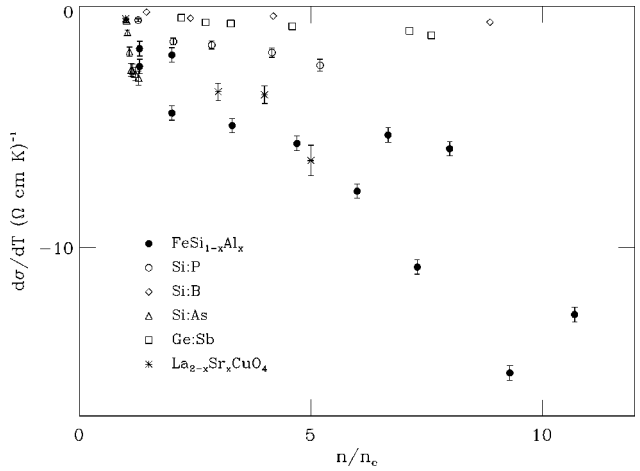

FIG. 20. First derivative of the conductivity with respect to temperature in the region of the linear $\sigma(T)$ for $FeSi_{1-x}Al_x$, Si:P (Ref. 21), Si:B (Ref. 21), Si:As (Refs. 38 and 21), Ge:Sb (Ref. 31), and $La_{2-x}Sr_xCuO_4$ (Refs. 58 and 59).

$La_{2-x}Sr_xCuO_4$.[58,59] Recent experiments at very high field have shown that the linear resistivity in $La_{2-x}Sr_xCuO_4$ does not continue down to zero temperature, just as in the classic doped semiconducting systems.[60] Similar to doped Si and FeSi, $La_{2-x}Sr-xCuO_4$ shows a strong upturn in ρ at low T and high fields. However, the form of the divergence in $La_{2-x}Sr-xCuO_4$ is logarithmic, perhaps reflecting the two-dimensional nature of the conduction in this anisotropic compound.

VI. DISCUSSION AND CONCLUSIONS

The experimental results presented in this paper taken as a whole reveal an insulator to metal transition for an Al concentration of $3.3(\pm 1.1)\times 10^{20}$ cm^{-3}. This is 2–3 orders of magnitude larger than the critical densities in Si:P and Ge:Sb of 3.87×10^{18} and 1.5×10^{17} cm^{-3}, respectively.[2,31] We have found no evidence that other types of order, such as superconducting, charge, or magnetic, appear nearby. The metal that results upon Al doping has a carrier mass which is nearly two orders of magnitude larger than that found in doped Si and Ge.[61] Furthermore, when we examine the low-temperature data in detail we find a MI transition that is quantitatively similar to that found in the classic semiconductors. There are only two substantial differences between our low-T data and that of doped Si and Ge. The first is the presence of SO or SF scattering in the majority of our samples, and the second is a slower divergence of the thermodynamic properties at low T.

We conclude from this set of experiments that the strong Coulomb effects in the Kondo insulator FeSi serve only to renormalize the critical density and the carrier mass in the metallic phase. Thus, by doping the ''exotic'' Kondo insulator FeSi, we find a garden variety doped semiconductor with a heavy mass—a heavy fermion metal. Our data lead us to the astonishing conclusion that this alloy made up of three of the most abundant elements (Fe, Si, and Al) is indeed a heavy fermion metal. Furthermore, there are few quantitative differences between the behavior of Si:P and this system near the MI transition which is a surprising conclusion given the significant mass enhancement. Because the interactions and disorder are both important in the description of the MI transition, it has remained an essentially unsolved problem.[1] We assert that the Mott-Anderson transition can be just as well investigated in FeSi as the classic semiconducting systems, since our data convincingly demonstrate that the same many-body physics determines the critical behavior.

In summary, we have carried out a systematic investigation of the transition from insulator to metal by carrier doping the Kondo insulator FeSi. We find a metal-insulator transition which is extraordinarily similar to that found in the classic semiconductors. It is surprising that the MI transition in a system where strong Coulomb effects dominate the behavior of the pure insulating system is quantitatively similar to that in the more conventional semiconductors. Our results suggest that many of the properties of systems near the MI transition are insensitive to the strength of the Coulomb effects in the pure insulating parent.

ACKNOWLEDGMENTS

We thank P. W. Adams, D. A. Browne, Z. Fisk, and D. R. Hamann for discussions. J. F. D. acknowledges the support of the Louisiana Board of Regents through Contract No. LEQSF(RF/1996-99)-RD-A-05 and the National Science Foundation under Grant No. DMR 97-02690.

[1] D. Belitz and T. R. Kirkpatrick, Rev. Mod. Phys. **66**, 261 (1994).
[2] T. F. Rosenbaum, R. F. Milligan, M. A. Paalanen, G. A. Thomas, R. N. Bhatt, and W. Lin, Phys. Rev. B **27**, 7509 (1983); P. Dai, Y. Zhang, and M. P. Sarachik, *ibid.* **45**, 3984 (1992).
[3] M. A. Paalanen, J. E. Graebner, R. N. Bhatt, and S. Sachdev, Phys. Rev. Lett. **61**, 597 (1988).
[4] D. B. McWhan, J. P. Remeika, J. P. Maita, H. Okinaka, K. Kosuge, and S. Kachi, Phys. Rev. B **7**, 326 (1973); S. A. Carter, T. F. Rosenbaum, P. Metcalf, J. M. Honig, and J. Spalek, *ibid.* **48**, 16 841 (1993).
[5] J. G. Bednorz and K. Muller, Z. Phys. B **64**, 189 (1986); B. Ellman, H. M. Jaeger, D. P. Katz, T. F. Rosenbaum, A. S. Cooper, and G. P. Espinosa, Phys. Rev. B **39**, 9012 (1989); N. W. Preyer, M. A. Kastner, C. Y. Chen, R. J. Birgeneau, and Y. Hidaka, *ibid.* **44**, 407 (1991); Y. Ando, G. S. Boebinger, A. Passner, T. Kimura, and K. Kishio, Phys. Rev. Lett. **75**, 4662 (1995); Y. Hidaka, Y. Tajima, K. Sugiyama, F. Tomiyama, A. Yamagashi, M. Date, and M. Hikita, J. Phys. Soc. Jpn. **60**, 1185 (1991).
[6] A. Husmann, D. S. Jin, Y. V. Zastavker, T. F. Rosenbaum, X. Yao, and J. M. Honig, Science **274**, 1874 (1996).
[7] J. F. DiTusa, K. Friemelt, E. Bucher, G. Aeppli, and A. P. Ramirez, Phys. Rev. Lett. **78**, 2831 (1997); **78**, 4309(E) (1997).
[8] K. Friemelt, J. F. DiTusa, E. Bucher, and G. Aeppli, Ann. Phys. (Leipzig) **5**, 175 (1996).
[9] G. Aeppli and Z. Fisk, Chem. Eng. Prog. **16**, 155 (1992); G. Aeppli, Z. Fisk, and J. F. DiTusa, in *Proceedings of the Workshop on Strongly Correlated Electronic Materials*, edited by K. S. Bedell, Z. Wang, D. Meltzer, A. V. Balatsky, and E. Abrahams (Addison-Wesley, Reading, 1994).
[10] Z. Fisk, J. L. Sarrao, J. D. Thompson, D. Mandrus, M. F. Hundley, A. Migliori, B. Bucher, Z. Schlesinger, G. Aeppli, E. Bucher, J. F. DiTusa, C. S. Oglesby, H.-R. Ott, P. C. Canfield, and S. E. Brown, Physica B **206 & 207**, 798 (1995).
[11] B. Bucher, Z. Schlesinger, P. C. Canfield, and Z. Fisk, Phys. Rev. Lett. **72**, 522 (1994).
[12] L. F. Mattheiss and D. R. Hamann, Phys. Rev. B **47**, 13 114 (1993); C. Fu, M. P. C. M. Krijn, and S. Doniach, *ibid.* **49**, 2219 (1994); C. Fu and S. Doniach, *ibid.* **51**, 17 439 (1995).
[13] V. Jaccarino, G. K. Wertheim, J. H. Wernick, L. R. Walker, and S. Arajs, Phys. Rev. **160**, 476 (1967).
[14] G. Shirane, J. E. Fischer, Y. Endoh, and K. Tajima, Phys. Rev. Lett. **59**, 351 (1987).
[15] V. I. Anisimov, S. Y. Ezhov, I. S. Elfimov, I. V. Solovyev, and T. M. Rice, Phys. Rev. Lett. **76**, 1735 (1996).
[16] Z. Schlesinger, Z. Fisk, Hai-Tao Zhang, M. B. Maple, J. F. DiTusa, and G. Aeppli, Phys. Rev. Lett. **71**, 1748 (1993).
[17] C.-H. Park, Z.-X. Shen, A. G. Loeser, D. S. Dessau, D. G. Mandrus, A. Migliori, J. Sarrao, and Z. Fisk, Phys. Rev. B **52**, 16 981 (1995).

[18] Ch. Kloc, E. Arushanov, M. Wendl, H. Hohl, U. Malang, and E. Bucher, J. Alloys Compd. **219**, 93 (1995).
[19] R. Wolfe, J. H. Wernick, and S. E. Haszko, Phys. Lett. **19**, 449 (1965).
[20] B. C. Sales, E. C. Jones, B. C. Chakoumakos, J. A. Fernandez-Baca, H. E. Harmon, J. W. Sharp, and E. H. Vdckmann, Phys. Rev. B **50**, 8207 (1994).
[21] P. W. Chapman, O. N. Tufte, J. D. Zook, and D. Long, J. Appl. Phys. **34**, 3291 (1963).
[22] T. Kurosawa, M. Matsui, and W. Sasaki, J. Phys. Soc. Jpn. **42**, 1622 (1977).
[23] K. Germanova, V. Donchev, V. Valchev, Ch. Hardalov, and I. Yanchev, Appl. Phys. A: Solids Surf. **50**, 369 (1990).
[24] A. Fert and P. M. Levy, Phys. Rev. B **36**, 1907 (1987).
[25] O. V. Emel'yanenko, T. S. Lagunova, D. N. Nasledov, and G. N. Talalakin, Fiz. Tverd. Tela (Leningrad) **7**, 1315 (1965) [Sov. Phys. Solid State **7**, 1063 (1965)].
[26] S. Takagi, H. Yasuoka, S. Ogawa, and J. H. Wernick, J. Phys. Soc. Jpn. **50**, 2539 (1981).
[27] M. B. Hunt, M. A. Chernikov, E. Felder, H. R. Ott, Z. Fisk, and P. Canfield, Phys. Rev. B **50**, 14 933 (1994).
[28] See, e.g., N. W. Ashcroft and N. D. Mermin, *Solid State Physics* (Saunders, Philadelphia, 1976).
[29] A. M. Finkel'stein, Zh. Éksp. Teor. Fiz. **84**, 168 (1983) [Sov. Phys. JETP **57**, 97 (1983)]; Sov. Sci. Rev., Sect. A **14**, 1 (1990); C. Castellani, G. Kotliar, and P. A. Lee, Phys. Rev. Lett. **59**, 323 (1987); T. R. Kirkpatrick and D. Belitz, *ibid.* **73**, 862 (1994); F. J. Wegner, Z. Phys. B **25**, 327 (1976).
[30] G. A. Thomas, Y. Ootuka, S. Kobayashi, and W. Sasaki, Phys. Rev. B **24**, 4886 (1981).
[31] S. B. Field and T. F. Rosenbaum, Phys. Rev. Lett. **55**, 522 (1985); Y. Ootuka, H. Matsuoka, and S. Kobayashi, in *Anderson Localization*, edited by T. Ando and H. Fukuyama (Springer-Verlag, Berlin, 1988); G. A. Thomas, A. Kawabata, Y. Ootuka, S. Katsumoto, S. Kobayashi, and W. Sasaki, Phys. Rev. B **26**, 2113 (1982).
[32] M. C. Maliepaard, M. Pepper, R. Newbury, and G. Hill, Phys. Rev. Lett. **61**, 369 (1988).
[33] D. J. Bishop, E. G. Spencer, and R. C. Dynes, Solid-State Electron. **28**, 73 (1985).
[34] A. T. Fiory and A. F. Hebard, Phys. Rev. Lett. **52**, 2057 (1984).
[35] B. L. Al'tshuler, A. G. Aronov, M. E. Gershenson, and Yu. V. Sharvin, Sov. Sci. Rev. Sect. A **9**, 223 (1987).
[36] P. A. Lee and T. V. Ramakrishnan, Rev. Mod. Phys. **57**, 284 (1985).
[37] G. Bergmann, Phys. Rep. **107**, 1 (1984).
[38] P. F. Newman and D. F. Holcomb, Phys. Rev. B **28**, 638 (1983).
[39] The weak-localization contribution in heavy fermion materials has been predicted to be enhanced by a factor of $\sqrt{m^*/m_e}$, J. W. Rasul, Phys. Rev. B **44**, 11 802 (1991).
[40] A. J. Millis and P. A. Lee, Phys. Rev. B **30**, 6170 (1984); **31**, 5523(E) (1985).
[41] A. A. Abrikosov and L. P. Gor'kov, Zh. Eksp. Teor. Fiz. **42**, 1088 (1962) [Sov. Phys. JETP **15**, 752 (1962)].
[42] G. Bergmann, Phys. Rev. B **28**, 515 (1983).
[43] G. Bergmann, Phys. Rev. Lett. **49**, 162 (1982).
[44] M. Sawicki, T. Dietl, J. Kossut, J. Igalson, T. Wojtowicz, and W. Plesiewicz, Phys. Rev. Lett. **56**, 508 (1986).
[45] M. P. Sarachik, A. Roy, M. Turner, M. Levy, D. He, L. L. Isaacs, and R. N. Bhatt, Phys. Rev. B **34**, 387 (1986).
[46] R. N. Bhatt and P. A. Lee, Phys. Rev. Lett. **48**, 344 (1982).
[47] R. N. Bhatt and D. S. Fisher, Phys. Rev. Lett. **68**, 3072 (1992).
[48] V. Dobrosavljevic, T. R. Kirkpatrick, and G. Kotliar, Phys. Rev. Lett. **69**, 1113 (1992).
[49] M. Lakner, H.v. Lohneysen, A. Langenfeld, and P. Wolffe, Phys. Rev. B **50**, 17 064 (1994).
[50] B. L. Al'tshuler, A. G. Aronov, and A. Yu. Zyuzin, Zh. Éksp. Teor. Fiz. **84**, 1525 (1983) [Sov. Phys. JETP **54**, 889 (1983)]; H. Fukuyama, J. Phys. Soc. Jpn. **50**, 3407 (1981).
[51] S. Ikehata and S. Kobayashi, Solid State Commun. **56**, 607 (1985); Y. Ootuka and N. Matsunaga, in *Anderson Localization*, edited by T. Ando and H. Fukuyama (Springer-Verlag, Berlin, 1987).
[52] H.v. Lohneysen, T. Pietrus, G. Portisch, H. G. Schlager, A. Schroder, M. Sieck, and T. Trappmann, Phys. Rev. Lett. **72**, 3262 (1994).
[53] M. A. Paalanen, S. Sachdev, R. N. Bhatt, and A. E. Ruckenstein, Phys. Rev. Lett. **57**, 2061 (1986).
[54] C. L. Seaman, M. B. Maple, B. W. Lee, S. Ghamaty, M. S. Torikachvili, J.-S. Kang, L. Z. Liu, J. W. Allen, and D. L. Cox, Phys. Rev. Lett. **67**, 2882 (1991).
[55] M. C. Aronson, R. Osborn, R. A. Robinson, J. W. Lynn, R. Chau, C. L. Seaman, and M. B. Maple, Phys. Rev. Lett. **75**, 725 (1995).
[56] O. O. Bernal, D. E. MacLaughlin, H. G. Lukefahr, and B. Andraka, Phys. Rev. Lett. **75**, 2023 (1995).
[57] E. Miranda, V. Dobrosavljevic, and G. Kotliar, Phys. Rev. Lett. **78**, 290 (1997).
[58] H. Takagi, B. Batlogg, H. L. Kao, J. Kwo, R. J. Cava, J. J. Krajewski, and W. F. Peck, Jr., Phys. Rev. Lett. **69**, 2975 (1992).
[59] S. L. Cooper, G. A. Thomas, A. J. Millis, P. E. Sulewski, J. Orenstein, D. H. Rapkine, S.-W. Cheong, and P. L. Trevor, Phys. Rev. B **42**, 10 785 (1990); W. E. Pickett, Rev. Mod. Phys. **61**, 433 (1989).
[60] G. S. Boebinger, Y. Ando, A. Passner, T. Kimura, M. Okuya, J. Shimoyama, K. Kishio, K. Tamasaku, N. Ichikawa, and S. Uchida, Phys. Rev. Lett. **77**, 5417 (1996).
[61] See, e.g., E. H. Putley, *The Hall Effect and Related Phenomena* (Butterworths, London, 1960).
[62] T. F. Rosenbaum, K. Andres, G. A. Thomas, and R. N. Bhatt, Phys. Rev. Lett. **45**, 1723 (1980); C. Yamanouchi, K. Mizuguchi, and W. Sasaki, J. Phys. Soc. Jpn. **22**, 859 (1967); Y. Ootuka, F. Komori, Y. Monden, S. Kobayashi, and W. Sasaki, Solid State Commun. **36**, 827 (1980).